

## Effects of hydrostatic pressure on the optic and transverse-acoustic vibrations of a (012) GaAs/AlAs superlattice

M. Holtz and T. Sauncy

*Department of Physics, Texas Tech University, Lubbock, Texas 79409*

K. Ploog\* and L. Tapfer

*Max-Planck-Institut für Festkörperforschung, Heisenbergstrasse 1, D-7000 Stuttgart 80, Germany*

(Received 20 May 1993)

We report on hydrostatic-pressure Raman measurements (to 2 GPa) of a superlattice composed of pure GaAs and pure AlAs grown in the (012) direction. We observe Raman and resonance-Raman scattering, where the resonance is achieved by pressure tuning the direct superlattice transition to match the excitation photon energy. The GaAs confined longitudinal and transverse optic modes are seen to resonate via the Fröhlich electron-phonon interaction. This is possible for the transverse mode due to mixing with the GaAs longitudinal-optical vibrations. Growth in this direction permits the observation of folded quasitransverse-acoustic phonons. The observation of these modes in first-order Raman scattering is supported by the weak pressure softening at a relative rate of  $-0.025 \pm 0.05 \text{ GPa}^{-1}$ , implying a mode-Grüneisen parameter of  $-1.9 \pm 0.4$  for the transverse-acoustic phonon.

### I. INTRODUCTION

Studies of superlattices typically address those grown with *c*-axis repetition along the conventional (001) crystal lattice direction. Measurements on superlattices with different growth orientations have been more sparse,<sup>1-3</sup> primarily due to difficulties encountered in their preparation. Popović *et al.*<sup>1,2</sup> have conducted Raman-scattering studies of (012) superlattices of GaAs and AlAs at ambient pressure. For this case, first-order Raman scattering is allowed by folded-acoustic phonons which are *primarily* transverse. Primarily relevant to this paper are two points. First, longitudinal- and transverse-acoustic modes which propagate along the (012) direction are permitted to mix. Hence, modes which are primarily transverse acoustic are designated quasitransverse (QT) and those which are primarily longitudinal are quasilongitudinal. Second, QT modes are allowed in first-order Raman scattering, permitting observation of transverse-acoustic phonons. The effect of pressure on folded longitudinal-acoustic phonons in (001) (GaAs)<sub>*n*</sub>(AlAs)<sub>*m*</sub> superlattices has been measured by Holtz, Syassen, and Ploog<sup>4</sup> but no measurements on folded transverse-acoustic phonons have been conducted.

In this paper, we report pressure-Raman measurements of the confined-optic and folded quasitransverse-acoustic vibrational modes of a GaAs/AlAs superlattice grown in the (012) direction. Measuring the pressure shift of the folded QT mode permits an assessment of the mode-Grüneisen parameter for transverse-acoustic vibrations for points in the bulk parent Brillouin zone which are neither at the zone center nor at the zone edge.

The intrinsic vibrational states of GaAs- and AlAs-based superlattices are readily classified into confined optic, folded acoustic, and interface phonons.<sup>5</sup> Optic phonons are confined due to the inability of the surrounding material (phonon barriers) to vibrate at the energies of

the material hosting the optic vibration. Confined modes which may be represented as standing waves within that material will have wave vectors.

$$k_m = \frac{m\pi}{(n+1)a}, \quad m = \pm 1, \pm 2, \dots, \quad (1)$$

with  $d = na$  the thickness of the layer to which the phonon is confined. The confining region consists of  $n$  monolayers with an atomic-monolayer-repeat distance of  $a = 1.263 \text{ \AA}$ . Wave functions of confined phonons with odd index  $m$  (*B* symmetry) are symmetric about a plane central to the material sheet to which the vibrations are confined, while those that are even  $m$  (*A* symmetry) are antisymmetric with respect to the same plane.

Folding of acoustic-phonon branches along the superlattice growth direction occurs due to the increased periodicity  $d_1 + d_2$ . This has the effect of reducing the size of (or folding) the Brillouin zone, mapping bulk acoustic phonons with wave vectors

$$k_m = \frac{2m\pi}{d_1 + d_2}, \quad m = 1, 2, \dots \quad (2)$$

back to the zone center, thus making them Raman active. For each index  $m$ , there are two acoustic branches at the zone center: one decreasing (denoted  $-m$ ) and the other increasing (denoted  $+m$ ) in energy as  $k_{\parallel}$  increases.

In bulk materials, the wave vector of the photon excitation and emission is so small that a  $k = \pm 4\pi n / \lambda \approx 0$  selection rule is employed [ $n = n(\lambda)$  is the index of refraction]. For superlattices, this  $\mathbf{k}$  is no longer negligible and can result in Raman allowed scattering far from the superlattice zone center.

We organize this paper in the following manner. After a description of the experiment, we report the effects of pressure on the optic phonons of the (012) superlattice, including the pressure tuned resonance Raman results. We then detail our results on the folded-acoustic vibra-

tional modes and discuss the implied mode-Grüneisen parameter.

## II. EXPERIMENTAL DETAILS

The superlattice studied here was grown on a (012) oriented pure GaAs substrate using molecular-beam epitaxy. Layers consisted of pure GaAs and pure AlAs, with thicknesses determined by double-crystal x-ray diffraction.<sup>1,2</sup> Our sample was composed of approximately 100 periods, each period being 14 monolayers of GaAs followed by 16 of AlAs.

In Fig. 1 we show the room-temperature, ambient pressure photoluminescence spectrum of our superlattice, generated with the 514.5-nm Ar<sup>+</sup> laser line. Between 1.4 and 1.5 eV we see the GaAs  $E_0$  band-gap emission originating from the underlying substrate. The emission from the lowest conduction-band state ( $n=1$ ,  $\Gamma$ -like) to the uppermost valence-band state ( $\Gamma$ -like, heavy hole) is also observed in the 1.8–1.9-eV range; both the conduction- and valence-band states in the superlattice have GaAs bulk parent states. The direct superlattice emission, denoted  $E_{hh}^I$ , has a maximum at energy 1.835 eV. The shift between the GaAs  $E_0$  and the superlattice  $E_{hh}^I$  is primarily due to confinement in the conduction and valence bands, and is depicted in the Fig. 1 inset. The inset shows the

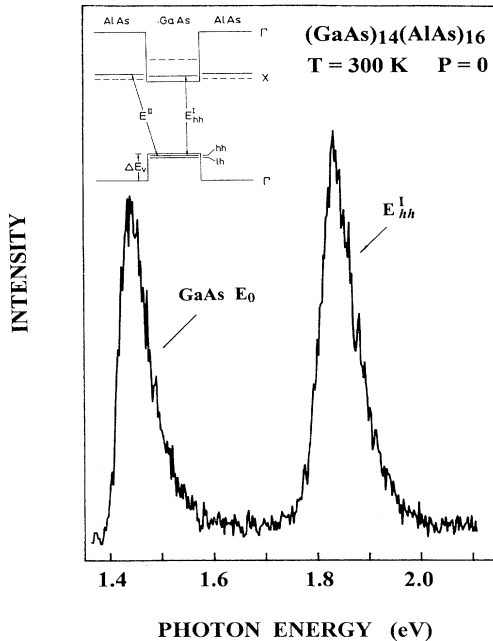


FIG. 1. Room-temperature photoluminescence spectrum of the (012) growth direction superlattice studied here. Seen are the GaAs substrate  $E_0$  emission and the superlattice  $E_{hh}^I$  emission. The confinement-induced shifting of the lowest-energy conduction-band states and the uppermost valence-band states is depicted for  $P=0$  in the inset for our superlattice which is near the type-I–type II crossover. The dashed lines in the inset are the  $X$ -like conduction-band levels; solid lines are for  $\Gamma$ -like states.

$P=0$  superlattice electronic energy-band structure vs growth direction. Here the  $\Gamma$ -like and  $X$ -like levels of the conduction band are drawn as solid and dashed lines, respectively, of the bulk materials, heavy lines are confined levels. The  $\sim 0.4$ -eV confinement-induced shift agrees well with what is expected from a simple envelope-function calculation. The spectrum in Fig. 1 verifies the high quality of our superlattice. The 1.835-eV energy level indicates that the lowest  $\Gamma$ -like conduction state is close in energy to the AlAs-like  $X$  minimum. The measured transition energy and the assumed pressure shift establish that the intensity enhancement we observe in our Raman measurements is an outgoing resonance with the superlattice  $E_{hh}^I$  transition. By  $P=0.5$  GPa the  $\Gamma$ -like state has shifted up in energy, and the minimum-energy conduction-band state is the  $X$ -like AlAs level.<sup>6,7</sup> At 0.5 GPa we observe substantially weakened emission from the superlattice. We made no attempt to determine if this was the  $E_{hh}^I$  line or the indirect  $E_{hh}^{II}$  luminescence. As the GaAs  $\Gamma$ -like state rapidly upshifts in energy, it crosses the AlAs  $X$ -like state. At this type-I–type-II crossover, the material becomes indirect and the emission is weak.<sup>6,8</sup>

For the pressure studies, substrates were then polished to produce a sample  $\sim 30$   $\mu\text{m}$  thick. These were then cleaved into small ( $\sim 100$ - $\mu\text{m}$  maximum length) segments, and loaded into a diamond-anvil cell along with a ruby for pressure calibration.<sup>9,10</sup> A 4:1 mixture of methanol and ethanol was used as a pressure-transmitting medium. We concern ourselves primarily with the relative pressure shifts  $[\partial(\ln\nu)/\partial P]_{P=0}$ , which are found to be more fundamental than the absolute pressure coefficient  $[\partial\nu/\partial P]_{P=0}$ .<sup>4</sup>

Raman (and photoluminescence) spectra were generated using the krypton ion 647.1-, 676.4-, and 568.2-nm laser lines, and the 514.5-nm line of an argon-ion laser. All spectra were recorded in the true backscattering geometry with incident and scattered light having parallel polarization. In order to accomplish the low Raman-shift measurements of the acoustic phonons, a triple-additive-dispersive system was constructed. This consisted of a 0.5-m monochromator to prefilter the light which was then passed to a 0.85-m double monochromator. These two were stepped synchronously in wavelength. The signal was measured using a cooled GaAs-photocathode photomultiplier in the photon-counting mode.

## III. OPTIC PHONONS UNDER PRESSURE

Figure 2 shows Raman spectra in the optic-phonon energy regime of the (012)  $(\text{GaAs})_{14}(\text{AlAs})_{16}$  superlattice. The lower spectrum is at ambient pressure and was generated using 568.2-nm (2.181-eV) excitation. This source is far from resonance with the  $E_{hh}^I$  transition in the superlattice. We observe confined longitudinal-optic phonons arising from both the GaAs and AlAs superlattice components. Also seen are internal superlattice interface vibrational modes, and confined transverse-optic modes. The spectrum is in good accord with that measured by Popović *et al.*, when we account for the fact that their

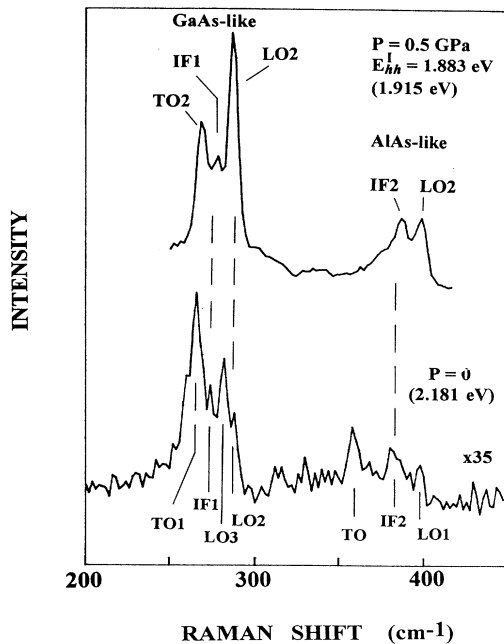


FIG. 2. Raman spectra (300 K) at zero pressure with 2.181-eV excitation (far from resonance) and at  $P=0.5$  GPa with 1.915-eV excitation (outgoing resonance with  $E_{hh}^1 = 1.883$  eV). Polarization of the incident and scattered light is parallel, with no attempt to orient the crystal.

measurements were at 80 K.<sup>1</sup> Relative pressure shifts of all optic-regime modes (GaAs- and AlAs-like confined optic, and interface) were found to be similar, with values of  $[\partial(\ln\nu)/\partial P]_{P=0} \approx 0.015$  GPa<sup>-1</sup>. These are also in good agreement with previous reports.<sup>4,11</sup>

The upper spectrum in Fig. 2 was obtained in resonance. Resonance was achieved by using the 647.1-nm (1.915-eV) laser line, and pressure shifting the  $E_{hh}^1$  transition energy into near resonance with the laser photon energy.<sup>11</sup> At a pressure of 0.5 GPa, the direct transition energy is near 1.883 eV (Ref. 5), producing outgoing-resonance conditions. The measured spectrum sits on the broad emission band (not shown) which exhibits about one-third the intensity of the strongest Raman band. An enhancement of the Raman signal by a factor of  $\sim 200$  is observed when compared with the nonresonant spectrum (same excitation source). The resonance-Raman spectrum in Fig. 2 shows even-index ( $A$ -symmetry) confined optic modes and the IF<sub>1</sub> and IF<sub>2</sub> interface modes to be enhanced, as anticipated.<sup>12,13</sup>

The strong band at 269 cm<sup>-1</sup> corresponds to a confined transverse-optic mode with  $m=2$  (even) index. This is concluded by comparing the zero-pressure, 80-K results of Popović *et al.*<sup>1</sup> with our results after accounting for the (assumed rigid) temperature difference and additional pressure shift of 2 cm<sup>-1</sup>. The assignment of this band as arising from GaAs-like TO phonons with  $m=2$  confinement index is also reasonable based on the anticipated selection rules when in resonance. Resonance here is via the Fröhlich electron-phonon mechanism, which does not usually apply for transverse-optic phonons. For

the (012) superlattice, however, the modes are not pure, and mixing of even (odd) transverse- and even (odd) longitudinal-optic phonons occurs. Thus, we observe Fröhlich-mechanism resonance enhancement of the  $m=2$  (even), primarily transverse-optic mode due to its admixing with the longitudinal-optic vibrations.

We note here that an alternative explanation for the TO-phonon enhancement is transparency-induced forward scattering.<sup>14</sup> Once the superlattice is transparent, and below the pressure at which the GaAs substrate is transparent to the excitation, the substrate will reflect a considerable amount of the incident light. Thus, forward Raman scattering is possible. This process may indeed contribute to our measured intensity, but since we do not observe an accompanying enhancement of the AlAs-like TO phonons, and because the intensity of the GaAs-like TO band returns to relative intensity levels similar to the  $P=0$  spectrum in Fig. 2, we support instead our resonance interpretation.

Interestingly, we do not observe an enhancement of the AlAs-like transverse-optic phonons. This is despite the fact that the  $\Gamma$ -like and  $X$ -like conduction-band states are nearly degenerate at 0.5 GPa. This indicates that most of the excited electronic state wave function is still confined to the GaAs layer, and therefore interacts more strongly with the phonons confined to the GaAs. This implies that at  $\Gamma$ - $X$  crossover there is no substantial mixing of the parent states at room temperature.

#### IV. TRANSVERSE-ACOUSTIC VIBRATIONS UNDER PRESSURE

Figure 3 exhibits low-frequency Raman spectra of the (012) (GaAs)<sub>14</sub>(AlAs)<sub>16</sub> superlattice at various pressures. Our primary observation is of the quasitransverse (QT) folded acoustic modes. The peak at  $29.1 \pm 0.2$  cm<sup>-1</sup> ( $P=0$ ) is identified as the QT(+1) upper-branch folded phonon after the first fold. This mode is primarily (98%) transverse.<sup>1</sup> The QT(+1) line also shows a strong resonance enhancement at  $P=0.5$  GPa. A much weaker feature is seen near  $18.4 \pm 0.3$  cm<sup>-1</sup>, which we identify as the QT(-1) mode based on the dispersion of the QT branch of this superlattice.<sup>1</sup> This line was difficult to resolve cleanly at low pressures due to competition with parasitic laser scattering. As the superlattice became transparent to the excitation (as seen in the  $P=2.1$  GPa spectrum in Fig. 3), the front-surface reflection diminished and the QT(-1) mode became easier to resolve. The  $\sim 11$ -cm<sup>-1</sup> splitting seen here is due to the large  $k$  vector of the 647.1-nm excitation. We find an effective speed of the QT wave propagation to be  $(3.31 \pm 0.03) \times 10^5$  cm/s, also in good agreement with Ref. 1.

Seen in the low-pressure spectrum in Fig. 3 is a weak feature at  $35.3 \pm 0.5$  cm<sup>-1</sup>. We attribute this to the first quasilongitudinal folded-acoustic phonon. This line was too weak in our spectra to reliably study under pressure.

As pressure increases, we find the expected weak redshift of the QT(+1) band, with an absolute rate of  $[\partial\nu/\partial P]_{P=0} = -0.73 \pm 0.14$  cm<sup>-1</sup>/GPa or at a relative

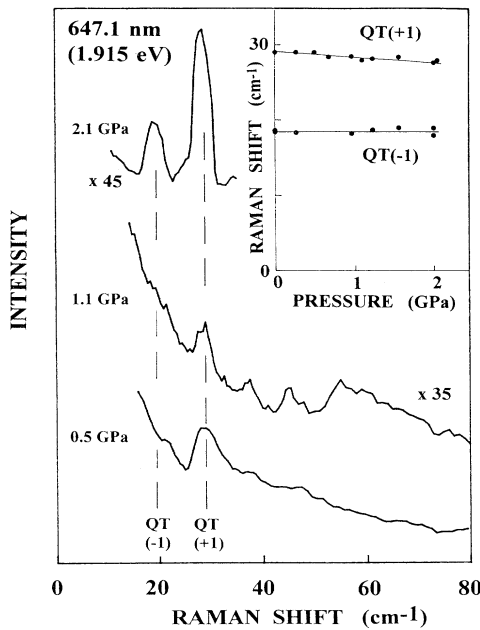


FIG. 3. Raman spectra of the (012)  $(\text{GaAs})_4(\text{AlAs})_{16}$  superlattice in the low-phonon-energy regime, taken with 647.1-nm excitation at various pressures. Dashed lines denote  $P=0$  energies of folded quasitransverse-acoustic modes ( $\text{QT}\pm 1$ ) obtained from linear fits to pressure data. The inset shows the progression of the two QT modes with pressure [the two  $\text{QT}(-1)$  points at 2.1 GPa were obtained using different laser photon energies]. Least-squares linear fits are shown.

rate of  $[\partial(\ln)\nu/\partial P]_{P=0} = -0.025 \pm 0.005 \text{ GPa}^{-1}$ . This pressure shift definitively proves that the feature we see originates from transverse-acoustic vibrations. The  $\text{QT}(-1)$  band has a very small relative shift ( $+0.005 \pm 0.010 \text{ GPa}^{-1}$ ). Given the difficulties in obtaining an accurate measure of the  $\text{QT}(-1)$  phonon energy at low pressure, we consider the  $\text{QT}(+1)$  measurement to be somewhat more reliable.

The (012) direction lies between the (001) and (011) zinc-blende crystal axes. The first folded-acoustic branch corresponds to a point in  $\mathbf{k}$  space close to the bulk material zone center with  $k \approx 0.07k_{\text{BZ}}$  (bulk). We will compare our results with the relative pressure coefficients of the bulk-GaAs transverse-acoustic (TA) zone edge  $\text{TA}(X)$  and  $\text{TA}(K)$  phonons.<sup>15</sup> The latter results are obtained from second-order pressure-Raman shifts. The  $\text{TA}(X)$

state has a relative pressure coefficient of  $-0.020 \text{ GPa}^{-1}$  while  $\text{TA}(K)$  shifts at a rate of  $-0.005 \text{ GPa}^{-1}$ . [For completeness,  $\text{TA}(L)$  has an accepted relative pressure coefficient of  $-0.020 \text{ GPa}^{-1}$ .] We find here that the relative pressure coefficient of the  $\text{QT}(+1)$  mode,  $-0.025 \pm 0.005 \text{ GPa}^{-1}$ , agrees best with the  $\text{TA}(X)$  relative shift.

We now turn our attention to the implied mode-Grüneisen parameter of the quasitransverse-acoustic phonon. The relative shifts measured for the  $\text{QT}(+1)$  mode yield a mode-Grüneisen parameter

$$\gamma_i = B_0 \left[ \frac{\partial \ln \nu}{\partial P} \right]_{P=0} \quad (3)$$

of  $\gamma_{\text{QT}(+1)} = -1.9 \pm 0.4$ . The superlattice  $B_0 = 76.8 \text{ GPa}$  represents an average of the GaAs bulk modulus (75.4 GPa, Ref. 16) and that of AlAs (78.1 GPa, Ref. 17). The large error stems primarily from the fact that we are measuring something small, which changes slowly.

Previous pressure studies of bulk semiconductors have always probed zone-center or zone-edge vibrations. The region of the Brillouin zone probed in our superlattice is neither zone center nor zone edge. The primary difference between previous measures of  $\gamma_{\text{TA}}$  is that we use first-order Raman scattering to measure an average property of GaAs and AlAs. Little is known about the latter, leaving us to compare our results with GaAs. At the bulk GaAs zone center,  $\gamma_{\text{TA}(\Gamma)}$  has been reported to be  $-0.05$ ,<sup>10</sup> which should be close to our current value. By way of further comparison, consider the  $\text{TA}(X)$  state. Reported  $\gamma_{\text{TA}(X)}$  values range from  $-1.2 \pm 0.1$  (Ref. 16) to  $-1.6$  (Ref. 13). Previous pressure-Raman measurements on superlattices yielded  $\gamma$ 's in excellent agreement with the accepted bulk crystal values. Our present value of  $\gamma_{\text{QT}(+1)} = -1.9 \pm 0.4$  implies slightly larger  $\gamma_{\text{TA}(X)}$  for AlAs than GaAs. Our measurement yields acceptable agreement given the experimental difficulties of these Raman measurements and the fact that little is known of the behavior of bulk AlAs. Further studies of superlattices with different periods would, however, yield both improved estimates and further details from within the Brillouin zone.

#### ACKNOWLEDGMENTS

The authors thank R. L. Lichti and U. D. Venkateswaran for thoroughly reading this manuscript.

\*Permanent address: Paul-Drude-Institut für Festkörperelektronik, O-1086 Berlin, Germany.

<sup>1</sup>Z. V. Popović, M. Cardona, E. Richter, D. Strauch, L. Tapfer, and K. Ploog, *Phys. Rev. B* **40**, 1207 (1989).

<sup>2</sup>Z. V. Popović, H. J. Trodahl, M. Cardona, E. Richter, D. Strauch, and K. Ploog, *Phys. Rev. B* **40**, 1202 (1989).

<sup>3</sup>V. Lemos, T. Ritter, and B. A. Weinstein, *Appl. Phys. Lett.* **61**, 1417 (1992).

<sup>4</sup>M. Holtz, K. Syassen, and K. Ploog, *Phys. Rev. B* **40**, 2988

(1989).

<sup>5</sup>B. Jusserand and M. Cardona, in *Light Scattering in Solids V*, edited by M. Cardona and G. Güntherodt (Springer, Berlin, 1989), Chap. 3.

<sup>6</sup>M. Holtz, R. Cingolani, K. Reimann, R. Muralidharan, K. Syassen, and K. Ploog, *Phys. Rev. B* **41**, 3641 (1990).

<sup>7</sup>M. Holtz, K. Syassen, R. Muralidharan, and K. Ploog, *Phys. Rev. B* **41**, 7647 (1990).

<sup>8</sup>U. D. Venkateswaran, M. Chandrasekhar, H. R. Chan-

- drasekhar, T. Wolfram, R. Fischer, W. T. Masselink, and H. Morkoç, *Phys. Rev. B* **31**, 4106 (1985).
- <sup>9</sup>G. J. Piermarini, S. Block, J. D. Barnett, and R. A. Forman, *J. Appl. Phys.* **46**, 2779 (1975).
- <sup>10</sup>B. A. Weinstein and R. Zallen, in *Light Scattering in Solids IV*, edited by M. Cardona and G. Güntherodt (Springer, Berlin, 1984), Chap. 8.
- <sup>11</sup>M. Holtz, U. D. Venkateswaran, K. Syassen, and K. Ploog, *Phys. Rev. B* **39**, 8458 (1989).
- <sup>12</sup>A. K. Sood, J. Menendez, M. Cardona, and K. Ploog, *Phys. Rev. Lett.* **54**, 2111 (1985).
- <sup>13</sup>A. K. Sood, J. Menendez, M. Cardona, and K. Ploog, *Phys. Rev. Lett.* **54**, 2115 (1985).
- <sup>14</sup>U. D. Venkateswaran, L. J. Cui, B. A. Weinstein, and F. A. Chambers, *Phys. Rev. B* **45**, 9237 (1992).
- <sup>15</sup>R. Trommer, H. Muller, M. Cardona, and P. Vogl, *Phys. Rev. B* **21**, 4869 (1980).
- <sup>16</sup>H. J. McSkimin, A. Jayaraman, and P. Andreatch, *J. Appl. Phys.* **38**, 2362 (1967).
- <sup>17</sup>S. Adachi, *J. Appl. Phys.* **58**, R1 (1985).